Article

Hexagonal-Close-Packed, Hierarchical Amorphous TiO Nanocolumn Arrays: Transferability, Enhanced Photocatalytic Activity, and Superamphiphilicity without UV Irradiation

Yue Li, Takeshi Sasaki, Yoshiki Shimizu, and Naoto Koshizaki

J. Am. Chem. Soc., **2008**, 130 (44), 14755-14762 • DOI: 10.1021/ja805077q • Publication Date (Web): 10 October 2008

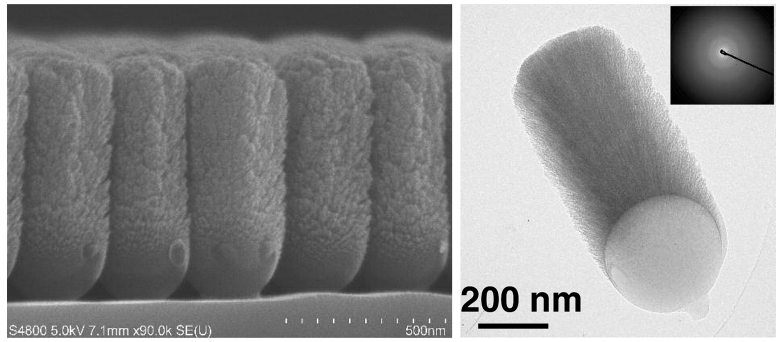

More About This Article

Additional resources and features associated with this article are available within the HTML version:

- Supporting Information
- Access to high resolution figures
- Links to articles and content related to this article
- Copyright permission to reproduce figures and/or text from this article

View the Full Text HTML

J|A|C|S
ARTICLES

Published on Web 10/10/2008

Hexagonal-Close-Packed, Hierarchical Amorphous TiO_2 Nanocolumn Arrays: Transferability, Enhanced Photocatalytic Activity, and Superamphiphilicity without UV Irradiation

Yue Li, Takeshi Sasaki, Yoshiki Shimizu, and Naoto Koshizaki*

Nanotechnology Research Institute (NRI), National Institute of Advanced Industrial Science and Technology (AIST), Central 5, 1-1-1 Higashi, Tsukuba, Ibaraki 305-8565, Japan

Received July 2, 2008; E-mail: koshizaki.naoto@aist.go.jp

Abstract: A hexagonal-close-packed (hcp), hierarchical amorphous TiO_2 nanocolumn array was fabricated by pulsed laser deposition (PLD) using a PS colloidal monolayer as a template under a high pressure (6.7 Pa) of background oxygen gas. The formation mechanism was investigated, and a model of multidirection glancing deposition was proposed to explain the formation process. This strategy can be extended to the fabrication of similar structures using different materials. Interestingly, this nanostructured array could be transferred to almost any substrate, avoiding restriction of substrate types in fabrication of nanocolumn arrays, which is helpful in the design and creation of nanodevices on various desired substrates. This hierarchical nanocolumn array exhibits excellent superamphiphilicity with both water and oil contact angles of 0°, without further UV irradiation. More importantly, the amorphous TiO_2 nanocolumn array demonstrates better performance in photocatalytic activity than an anatase nanocolumn array due to its large surface area and special microstructures, suggesting that the surface area of the TiO_2 is preferable to its crystal structure for enhancing photocatalytic activity. The combination of superamphiphilicity and photocatalytic activity gives the surface an excellent self-cleaning effect.

Introduction

Nanostructured ordered arrays have recently attracted much interest due to their applications in photonic crystals,[1] active substrates for surface-enhanced Raman spectroscopy,[2] biosensors,[3] microfluidic devices,[4] and so forth. The conventional methods for obtaining nanostructured arrays are lithographic techniques including optical lithography,[5a] X-ray lithography,[5b] electron-beam lithography,[5c] and soft lithography.[5d] For these methods, in which corresponding masks must be prepared in order to fabricate nanoarrays with different morphologies, the problems of high cost and low throughput remain unsolved, and therefore, most laboratories cannot afford these technologies. Recently, other parallel techniques, mainly based on self-assembling routes, have been developed.[6] One of these methods, the monolayer colloidal crystal template technique (also called colloidal monolayer lithography), has proved to be a successful and promising technique.[7] By using this strategy and taking the monolayer colloidal crystal as a mask or template, nanoparticle arrays,[8] nanopore arrays,[9] nanoring arrays,[10] and even one-dimensional nanostructured arrays[11] including nanotubes,[11a,b] nanopillars,[11c,d] and nanowire arrays[11e] could be prepared. Although this technique is well developed, there is still an interest in devising novel nanostructured arrays by combining the colloidal monolayer with other techniques (e.g., electron-beam irradiation, sputtering, pulsed laser deposition, etc). Furthermore, many investigations have recently demonstrated that hierarchical structures could improve the properties of materials in optoelectronic devices, biomedical science, field emission, bionic superhydrophobic surfaces, and so forth,[12] and therefore, these have attracted much attention.

Here, we present a new approach for fabricating hierarchical nanocolumn arrays by pulsed laser deposition (PLD) using a polystyrene (PS) colloidal monolayer as a template. In this

(1) (a) Poborchii, V.; Tada, T.; Kanayama, T. *Appl. Phys. Lett.* **1999**, *75*, 32. (b) Duan, G.; Cai, W.; Luo, Y.; Sun, F. *Adv. Funct. Mater.* **2007**, *17*, 644.
(2) (a) Haynes, C. L.; Van Duyne, R. P. *J. Phys. Chem. B* **2003**, *107*, 7426. (b) Duan, G. T.; Cai, W. P.; Luo, Y. Y.; Li, Y.; Lei, Y. *Appl. Phys. Lett.* **2006**, *89*, 181918.
(3) Haes, A. J.; Van Duyne, R. P. *J. Am. Chem. Soc.* **2002**, *124*, 10596.
(4) Blossey, R. *Nat. Mater.* **2003**, *2*, 301.
(5) (a) Wallraff, G. M.; Hinsberg, W. D. *Chem. Rev.* **1999**, *99*, 1801. (b) Smith, H. I.; Schattenburg, M. L. *IBM J. Res. Develop.* **1993**, *37*, 319. (c) Ito, T.; Okazaki, S. *Nature* **2000**, *406*, 1027. (d) Xia, Y. N.; Whitesides, G. M. *Angew. Chem., Int. Ed.* **1998**, *37*, 550.
(6) Wang, Z. L. *Adv. Mater.* **1998**, *10*, 13.
(7) (a) Yang, S.-M.; Jang, S. G.; Choi, D.-G.; Kim, S.; Yu, H. K. *Small* **2006**, *2*, 458. (b) Li, Y.; Cai, W. P.; Duan, G. T. *Chem. Mater.* **2008**, *20*, 615.
(8) Malinsky, M. D.; Kelly, L.; Schatz, G. C.; Van Duyne, R. P. *J. Am. Chem. Soc.* **2001**, *123*, 1471.
(9) (a) Jiang, P. *Angew. Chem., Int. Ed.* **2004**, *43*, 5625. (b) Li, Y.; Cai, W. P.; Cao, B. Q.; Duan, G. T.; Li, C. C.; Sun, F. Q.; Zeng, H. B. *J. Mater. Chem.* **2006**, *16*, 609. (c) Lu, Z. X.; Namboodiri, A.; Collinson, M. M. *ACS Nano* **2008**, *2*, 993.
(10) Sun, F. Q.; Yu, J. C.; Wang, X. C. *Chem. Mater.* **2006**, *18*, 3774.
(11) (a) Tu, Y.; Lin, Y.; Ren, Z. F. *Nano Lett.* **2003**, *3*, 107. (b) Kempa, K.; Kimball, B.; Rybczynski, J.; Huang, Z. P.; Wu, P. F.; Steeves, D.; Sennett, M.; Giersig, M.; Rao, D. V. G. L. N.; Carnahan, D. L.; Wang, D. Z.; Lao, J. Y.; Li, W. Z.; Ren, Z. F. *Nano Lett.* **2003**, *3*, 13. (c) Liu, D. F.; Xiang, Y. J.; Wu, X. C.; Zhang, Z. X.; Liu, L. F.; Song, L.; Zhao, X. W.; Luo, S. D. W.; Ma, J.; Shen, J.; Zhou, W. Y.; Wang, G.; Wang, C. Y.; Xie, S. S. *Nano Lett.* **2006**, *6*, 2375. (d) Li, Y.; Cai, W. P.; Cao, B. Q.; Duan, G. T.; Sun, F. Q. *Polymer* **2005**, *46*, 12033. (e) Wang, X. D.; Summers, C. J.; Wang, Z. L. *Nano Lett.* **2004**, *4*, 423.

method, the monolayer PS colloidal crystal was fabricated on the substrate and used as a template. The desired material is then deposited on it by PLD at room temperature, using oxygen as the background gas. This nanocolumn array has a special hierarchical structure with a hexagonal-close-packed (hcp) arrangement. The nanocolumn stands vertically on the PS sphere tops, and nanobranches in each nanocolumn grow in a radiation-like manner, perpendicular to the PS sphere surface. Importantly, such a nanocolumn array can be transferred to any desired substrate (e.g., TEM copper grid) and still keep its integrity, even when picking it up using another substrate when the PS colloidal monolayer is being dissolved in an organic solution. This transferability avoids restriction of substrate types in the fabrication process for nanocolumn arrays, which is helpful for the design and fabrication of new nanodevices.

TiO_2 is a very useful functional material due to its wide application in the fields of photocatalysis,[13] optical materials,[14] dye-sensitized solar cells,[15] lithium-ion batteries,[16] and superhydrophobic[17] and superhydrophilic materials.[18] We demonstrated the synthesis of hcp hierarchical nanocolumn arrays on the substrate using the strategy presented here and by taking TiO_2 as an example and investigated the growth mechanism of nanocolumn arrays. Besides TiO_2, similar nanocolumn arrays of other materials including SnO_2, Fe_2O_3, and carbon can also be fabricated by the presented strategy. Interestingly, prepared amorphous TiO_2 nanocolumn arrays exhibit a strong superamphiphilicity with contact angles of 0° for both water and oil, and enhanced photocatalytic activity for organic materials, which has important applications in self-cleaning surfaces.

Experimental Section

A 2.5 wt% suspension of monodispersed polystyrene (PS) spheres with a diameter of 350 nm was purchased from Alfa Aesar. The PS colloidal monolayers were first fabricated on cleaned Si substrates by spin coating. A droplet of PS sphere suspension was placed on a cleaned substrate with an area of 15×15 mm^2 fixed on a spin coater at a rotating speed of 800 rpm for 5 min. A colloidal monolayer with an area of about 2 cm^2 was formed on the substrate by a self-assembling process.[19]

The colloidal monolayer with its supporting substrate was placed in a deposition chamber, close to the target and at an off-axial position with respect to the target (Figure S1 of the Supporting Information). A laser beam with a wavelength of 355 nm from a Q-switched Nd:YAG laser (Continuum, Precision 8000), operated at 10 Hz with 100 mJ/pulse and a pulse width of 7 ns was applied and focused on the target surface with a diameter of 2 mm. Rutile titanium dioxide was used as the target. The substrate and target were rotated at 40 and 30 rpm, respectively. PLD was carried out at a base pressure of 2.66×10^{-4} Pa and a background O_2 pressure of 6.7 Pa.

Photocatalytic experiments of TiO_2 nanocolumn arrays were conducted as follows. The as-prepared samples were immersed in a 20 mM stearic acid ethanol solution for 12 h and then taken out for drying at room temperature. The stearic acid molecules were adsorbed onto the sample surface. The as-prepared samples with stearic acid were then directly irradiated with UV light at ambient atmosphere. The UV light was supplied by a SLUV-6 light source with a wavelength of 254 nm and a power of 90 W (or light intensity of 1.27 W cm^{-2}). The decomposition of stearic acid during UV illumination was investigated by measuring the decay of the infrared peaks for the symmetric and asymmetric vibrations of the CH_2 using a FTIR spectrometer (JASCO FT-IR 420) in a diffuse reflectance mode.

The morphologies of the as-prepared samples were observed by a field emission scanning electron microscope (FE-SEM, Hitachi S-4800) and a transmission electron microscope (TEM, JEOL TEM-2010). The composition and chemical states of the samples were examined by X-ray photoelectron spectroscopy (XPS, PHI, 5600ci). The water contact angle (CA) was measured with a VCA Optima XE from AST Products Inc.

Results and Discussion

Figure 1 presents FE-SEM images of the sample obtained by PLD using the PS colloidal monolayer with sphere size of 350 nm. It can be clearly seen that an ordered nanocolumn array with a hexagonal-close-packed arrangement was synthesized (Figure 1a). Each nanocolumn is composed of two parts: a PS sphere at the bottom and a vertical nanocolumn on the top of the PS sphere (Figure 1b). The diameter of the nanocolumn was almost the same as that of the PS sphere, and its height was about 870 nm. The nanocolumn had a very rough structure on the surface and seemed to be composed of many nanobranches, according to the high-resolution images of the side view (Figure 1 c, d).

The corresponding TEM results are presented in Figure 2. Observation from the top of the nanocolumn arrays indicates

(12) (a) Morariu, M.; Voicu, N.; Schäffer, E.; Lin, Z.; Russell, T. P.; Steiner, U. *Nat. Mater.* **2003**, *2*, 48. (b) Ye, C. H.; Zhang, L. D.; Fang, X. S.; Wang, Y. H.; Yan, P.; Zhao, J. W. *Adv. Mater.* **2004**, *16*, 1019. (c) Gao, P. X.; Ding, Y.; Wang, Z. L. *Nano. Lett.* **2003**, *3*, 1315. (d) Meng, G. W.; Jung, Y. J.; Cao, A. Y.; Vajtai, R.; Ajayan, P. M. *Proc. Natl. Acad. Sci. U. S. A.* **2005**, *102*, 7074. (e) Cho, S. O.; Lee, E. J.; Lee, H. M.; Kim, J. G.; Kim, Y. J. *Adv. Mater.* **2006**, *18*, 60. (f) Li, Y.; Li, C. C.; Cho, S. O.; Duan, G. T.; Cai, W. P. *Langmuir* **2007**, *23*, 9802.

(13) (a) Hoffmann, M. R.; Martin, S. T.; Choi, W.; Bahnemann, D. W. *Chem. Rev.* **1995**, *95*, 69. (b) Fujishima, A.; Honda, K. *Nature* **1972**, *238*, 37. (c) Zhou, Y.; Antonietti, M. *J. Am. Chem. Soc.* **2003**, *125*, 14960. (d) Zhou, Y.; Ma, R. Z.; Ebina, Y.; Takada, K.; Sasaki, T. *Chem. Mater.* **2006**, *18*, 1235. (e) Tang, J. W.; Quan, H. D.; Ye, J. H. *Chem. Mater.* **2007**, *19*, 116. (f) Yang, P.; Yang, M.; Zou, S. L.; Xie, J. Y.; Yang, W. T. *J. Am. Chem. Soc.* **2007**, *129*, 1541.

(14) Tang, H.; Berger, H.; Schmid, P. E.; Lévy, F. *Solid State Commun.* **1993**, *87*, 847.

(15) (a) Oregan, B.; Grätzel, M. *Nature* **1991**, *353*, 737. (b) Wang, Z. S.; Huang, C. H.; Huang, Y. Y.; Hou, Y. J.; Xie, P. H.; Zhang, B. W.; Cheng, H. M. *Chem. Mater.* **2001**, *13*, 678. (c) Papageorgiou, A. C.; Pang, C. L.; Chen, Q.; Thornton, G. *ACS Nano* **2007**, *1*, 409. (d) Kuang, D.; Brillet, J.; Chen, P.; Takata, M.; Uchida, S.; Miura, H.; Sumioka, K.; Zakeeruddin, S. M.; Grätzel, M. *ACS Nano* **2008**, *2*, 1113.

(16) (a) Zhou, H. S.; Li, D. L.; Hibino, M.; Honma, I. *Angew. Chem., Int. Ed.* **2005**, *44*, 797. (b) Hosono, E.; Fujihara, S.; Imai, H.; Honma, I.; Masaki, I.; Zhou, H. S. *ACS Nano* **2007**, *1*, 273.

(17) (a) Feng, X.; Zhai, J.; Jiang, L. *Angew. Chem., Int. Ed.* **2005**, *44*, 5115. (b) Zhang, X. T.; Kono, H.; Liu, Z. Y.; Nishimoto, S.; Tryk, D. A.; Murakami, T.; Sakai, M.; Fujishima, A. *Chem. Commun.* **2007**, 4949. (c) Zhang, X. T.; Jin, M.; Liu, Z. Y.; Tryk, D. A.; Nishimoto, S.; Murakami, T.; Fujishima, A. *J. Phys. Chem. C* **2007**, *111*, 658.

(18) (a) Miyauchi, M.; Nakajima, A.; Fujishima, A.; Hashimoto, K.; Watanabe, T. *Chem. Mater.* **2000**, *12*, 3. (b) Sakai, N.; Fujishima, A.; Watanabe, T.; Hashimoto, K. *J. Phys. Chem. B* **2001**, *105*, 3023. (c) Hosono, E.; Matsuda, H.; Honma, I.; Ichihara, M.; Zhou, H. S. *Langmuir* **2007**, *23*, 7447. (d) Wang, R.; Sakai, N.; Fujishima, A.; Watanabe, T.; Hashimoto, K. *J. Phys. Chem. B* **1999**, *103*, 2188. (e) Miyauchi, M.; Tokudome, H. *Appl. Phys. Lett.* **2007**, *91*, 043111. (f) Gu, Z. Z.; Fujishima, A.; Sato, O. *Appl. Phys. Lett.* **2004**, *85*, 5067. (g) Wu, Z.; Lee, D.; Rubner, M. F.; Cohen, R. E. *Small* **2007**, *3*, 1445. (h) Li, Y.; Sasaki, T.; Shimizu, Y.; Koshizaki, N. Small, in press.

(19) (a) Yan, X.; Yao, J.; Lu, G.; Li, X.; Zhang, J.; Han, K.; Yang, B. *J. Am. Chem. Soc.* **2005**, *127*, 7688. (b) Zhang, G.; Wang, D. Y.; Gu, Z. Z.; Möhwald, H. *Langmuir* **2005**, *21*, 9143. (c) Zhang, G.; Wang, D. Y.; Möhwald, H. *Angew. Chem., Int. Ed.* **2005**, *44*, 7767. (d) Xu, H.; Goedel, W. A. *Small* **2005**, *1*, 808. (e) Li, Y.; Huang, X. J.; Heo, S. H.; Li, C. C.; Choi, Y. K.; Cai, W. P.; Cho, S. O. *Langmuir* **2007**, *23*, 2169. (f) Ctistis, G.; Patoka, P.; Wang, X.; Kempa, K.; Giersig, M. *Nano Lett.* **2007**, *7*, 2926. (g) Rybczynski, J.; Ebels, U.; Giersig, M. *Colloids Surf., A* **2003**, *219*, 1. (h) Kosiorek, A.; Kandulski, W.; Glacynska, H.; Giersig, M. *Small* **2005**, *1*, 439. (i) Li, Y.; Lee, E. J.; Cai, W.; Kim, K. Y.; Cho, S. O. *ACS Nano* **2008**, *2*, 1108.

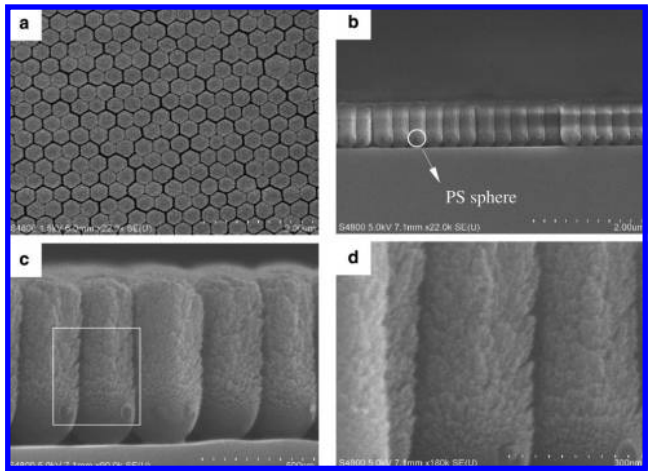

Figure 1. FE-SEM images of a sample obtained by PLD using a PS colloidal monolayer as the substrate (PS sphere size: 350 nm; deposition time: 70 min). (a) and (b) are low-magnification images observed from the top and side. (c) and (d) are high-resolution images observed from the side. (d) is an expanded image of (c).

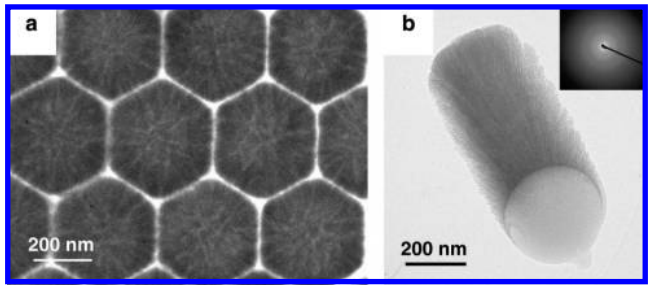

Figure 2. TEM images of the sample depicted in Figure 1. The nanocolumns were scraped from the substrate with a scalpel and transferred onto the TEM grid for TEM observation. (a) Ordered nanocolumn array observed from the top. (b) Single nanocolumn observed from the side. The inset in (b) is the corresponding electron diffraction pattern.

that each nanocolumn consists of radiation-shaped nanobranches emanating from the center (Figure 2a). The image of a single isolated nanocolumn clearly shows that the nanocolumn is composed of a PS sphere and a nanocolumn on the sphere surface. The nanocolumn has nanobranch-structures, which grow almost vertically on the surface of the sphere (Figure 2b). The nanobranch-structures indicate that the nanocolumn possesses a hierarchical, porous structure and hence has a high surface area. The selected area electron diffraction (SAED) pattern seen in the inset demonstrates that the nanobranches deposited on PS spheres by PLD are amorphous.

The XPS spectrum for the as-prepared sample indicates that the elements of titanium, oxygen, and carbon were detected (Figure 3). Ti and O should originate from the nanocolumn, and the atomic ratio of Ti and O was about 1:2, which corresponded well to the target of the PLD process. Carbon originating from impurities in the air is always detected in XPS measurement. The SAED pattern and XPS results indicate that the nanocolumn on the PS sphere is amorphous TiO_2.

Formation Mechanism of hcp Hierarchical Nanocolumn Arrays. If a higher rotation speed (2000 rpm) and lower concentration (1.0 wt%) of PS colloidal microsphere suspension were used in fabricating a colloidal monolayer by spin-coating, it will be difficult to form a monolayer colloidal crystal with a large area; however, a single colloidal microsphere or microsphere-clusters with varying numbers (2, 3, 4,...) of spheres can

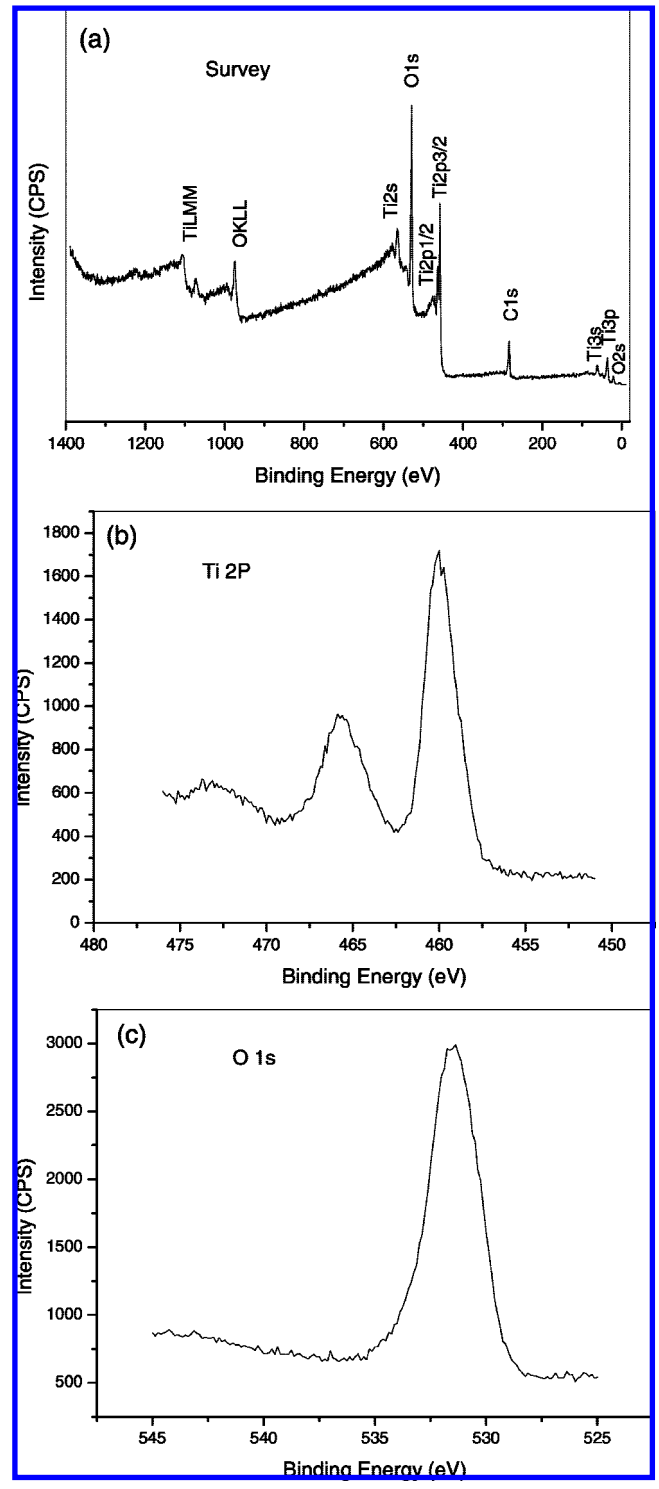

Figure 3. XPS spectra of nanocolumn arrays. (a) is the survey spectrum; (b) and (c) are spectra from Ti 2p and O 1s core levels.

be easily found on the substrate, as indicated in column A of Table 1. After deposition by PLD, morphologies observed from the top changed from those seen before PLD, as indicated in column B of Table 1. For a single PS microsphere, we can see that the shape maintained spherical but that the size increased from 350 nm (PS sphere size) to 500 nm after PLD. Interestingly, for the microsphere-clusters with spheres numbering from two to six, each unit in the sphere-cluster still increased in size, but could not retain the spherical shape after PLD. Growth was

Table 1. Morphologies of before and after PLD on the PS Sphere Surface (Scale Bars are 500 nm)

Number of PSs	(A) Before PLD	(B) After PLD
One	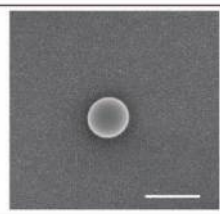	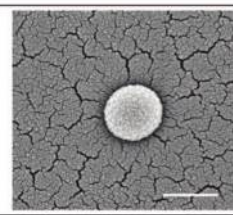
Two	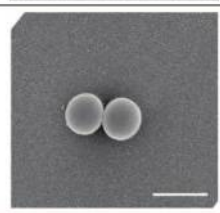	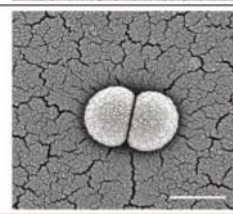
Three	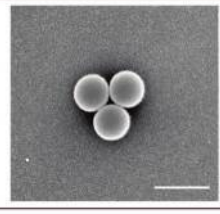	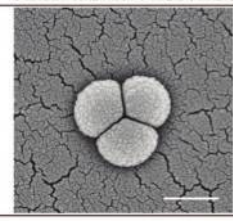
Four	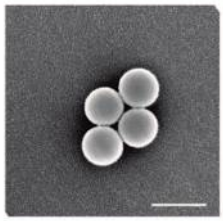	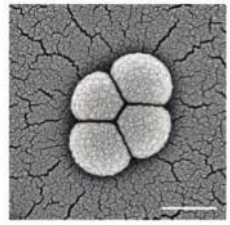
Five	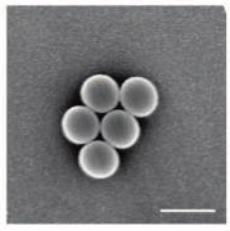	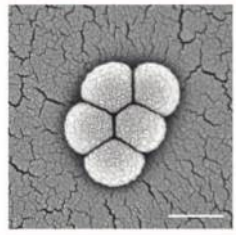
Six	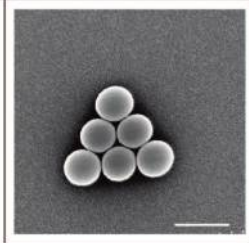	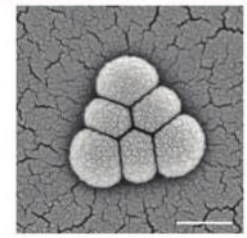
Seven	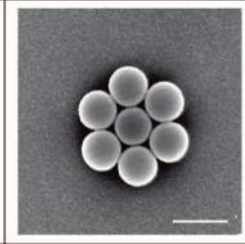	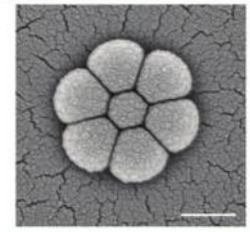
Ten	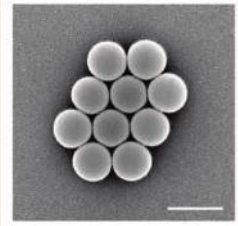	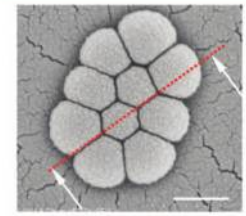 Observation from top 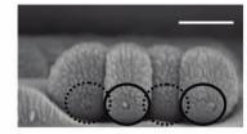 Section view along the red dot line

restricted at the contact point of two neighboring units, with the contact between the neighboring units changing from a quasidot contact to a facet contact before (sphere-cluster) and after (sphere-cluster with coating on the surface) PLD. If a sphere in sphere-cluster was completely surrounded by others, for example, the center sphere in a sphere-cluster of seven with a hexagonal close packed (hcp) arrangement, its size after deposition was nearly the same as before PLD and only the morphology was slightly changed from spherical to hexagonal. If we observe a section of a sphere-cluster of 10 spheres with hcp arrangement after PLD, we can clearly see that nanocolumns have formed on the two spheres completely surrounded by the others and that nanocolumns cannot be formed on the spheres at the edge of the sphere-cluster. This implies that a nanocolumn array will be easily formed after PLD if a monolayer colloidal crystal with a large area is used in the PLD process.

In addition, if we deposit the desired materials using a bare silicon substrate without any PS spheres by PLD, we find that nanocolumns grow vertically on the substrate, as seen in Figure 4. Generally, nanocolumns prefer to grow in the normal direction during the PLD process.[20]

In the PLD process, the desired target (TiO_2) is irradiated by a laser beam using an energy level exceeding its threshold in vacuum environment, ions (Ti^{4+}, O^{2-}, etc.) and electrons are released into the chamber from the target along the target normal. However, if a background gas with high pressure is introduced into the chamber, the movement direction will be changed from an almost uniform direction to multidirection due to collisions between the ions, electrons, and molecules of the ejected species and the background gas.

Combining the above results, we can easily understand the formation mechanism of hierarchical hcp nanocolumn arrays, as demonstrated in Scheme 1. If a bare substrate is used in the PLD process, a film composed of vertical nanocolumns of small diameter will be formed. If a single PS sphere is on the substrate,

(20) (a) Sun, Y.; Addison, K. E.; Ashfold, M. N. R. *Nanotechnology* **2007**, *18*, 495601. (b) Solanki, R.; Huo, J.; Freeouf, J. L.; Miner, B. *Appl. Phys. Lett.* **2002**, *81*, 3864.

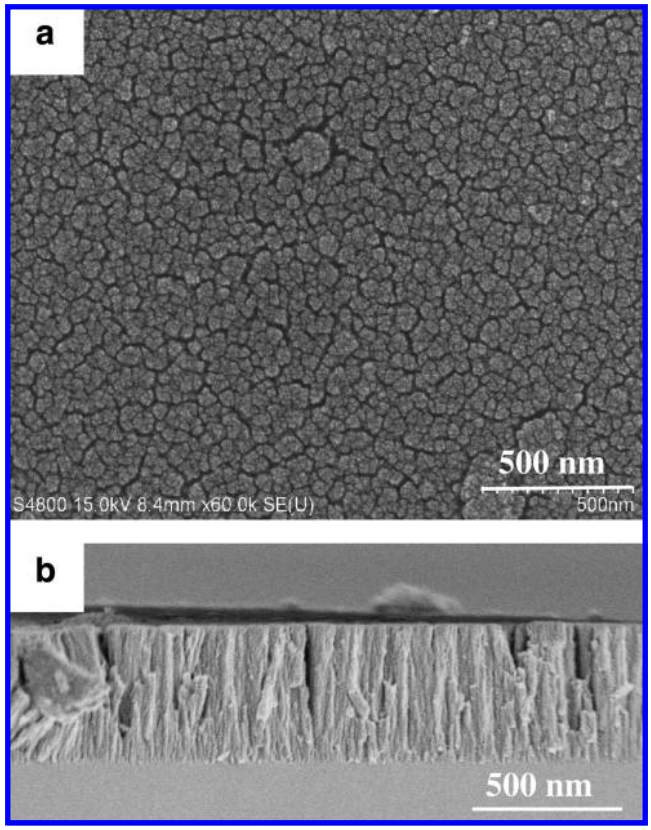

Figure 4. FE-SEM images of the TiO_2 deposit obtained by PLD directly on a bare substrate without using colloidal spheres. (a) Observation from top. (b) Section view.

Scheme 1. Schematic Illustration of Formation Mechanism of hcp Nanocolumn Arrays

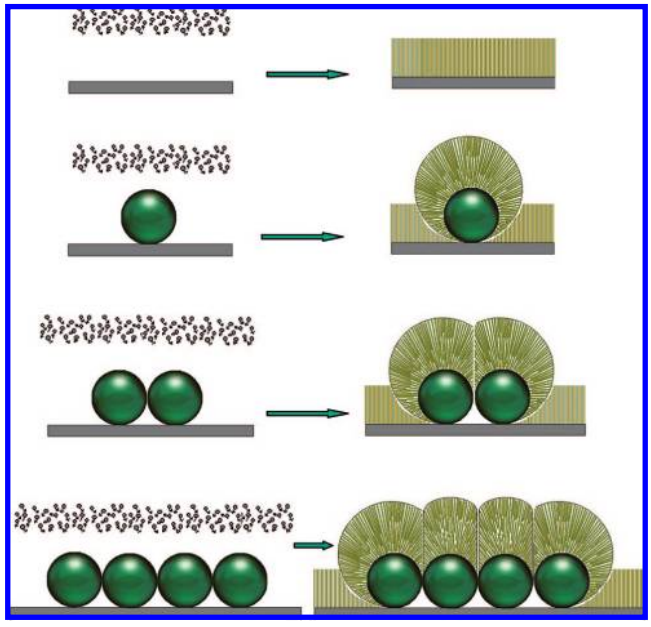

a composite of a PS sphere at the bottom and a shell composed of radiation-shaped nanobranches on top of the sphere will appear, due to preferential vertical growth along the normal direction of the supporting surface and multidirectional deposition. For a sphere cluster (more than one sphere) on the substrate, a shadow effect will be produced in the deposition between any two neighboring spheres. If one sphere in the sphere-cluster is completely surrounded by six other spheres as in the case of hcp alignment, one nanocolumn will be produced on the top of this sphere. If a monolayer colloidal crystal with cm^2-sized area is adopted, this strategy can easily produce an hcp nanocolumn array.

In this experiment, we adopted an off-axis configuration where the target and substrate are perpendicularly placed. This configuration is similar to the glancing angle deposition (GLAD) or oblique angle deposition in which there is a large angle between the deposition direction and the normal direction of the substrate.[21] In the traditional GLAD technique, atoms from the target obliquely arrive and condense on the substrate, and the tilted and separated nanowires or nanopillars having a porous structure are gradually formed due to the shadowing effect of the initial deposits under high-vacuum conditions.[21] The critical difference between our experiment and GLAD is the ambient pressure during deposition, which converts the directional flow of ejected species in a vacuum into a multidirectional flow at higher pressure. Therefore, the multidirection deposition caused by the high pressure of the background gas is a principal reason why a vertical nanocolumn array with hcp alignment is formed on the colloidal monolayer. This can be further verified by changing the angles between substrates and target after PLD, as seen in Figures S2 and S3 of the Supporting Information. If these experiments were carried out in a vacuum, tilted nanocolumns with different angles would be obtained on the different substrates. However, from our results, we can see that the nanocolumn morphologies are independent of the angle between the substrate and target but the growth rates are different for different angles because of the plume shape in PLD (Figure S3 of the Supporting Information).

Besides TiO_2 amorphous hcp nanocolumn arrays, the presented strategy can be extended to the fabrication of similar structures of SnO_2, Fe_2O_3, C, and so forth, just by changing the corresponding target in the PLD process.

Transferability. The as-prepared nanocolumns in an ordered array are each composed of a PS sphere at the bottom and a nanocolumn on the top of the PS sphere. If the PS colloidal monolayer is dissolved by an organic solution (CH_2Cl_2), this ordered nanocolumn array could retain its integrity while being peeled from the substrate due to the van der Waals force between the neighboring nanocolumns suspended in the solution. It could then be transferred to any desired substrate (e.g., TEM copper grid) by picking it up using another substrate, as illustrated in Scheme 2 and Figure 5. The transferability avoids restrictions on substrates in the fabrication process of TiO_2 nanocolumn arrays, which is helpful in the design and fabrication of new nanodevices on any desired substrates.

Superamphiphilicity without UV Irradiation. The investigation of wettability indicates that the as-prepared TiO_2 nanocolumn array exhibited strong superamphiphilicity. Contact angles for both water and oil (rapeseed oil) were 0°. When we dropped

(21) (a) Brett, M. J.; Hawkeye, M. M. *Science* **2008**, *319*, 1192. (b) Robbie, K.; Beydaghyan, G.; Brown, T.; Dean, C.; Adams, J.; Buzea, C. *Rev. Sci. Instrum.* **2004**, *75*, 1089. (c) Zhao, Y.-P.; Ye, D.-X.; Wang, G.-C.; Lu, T.-M. *Nano Lett.* **2002**, *2*, 351. (d) Hrudey, P. C. P.; Szeto, B.; Brett, M. J. *Appl. Phys. Lett.* **2006**, *88*, 251106. (e) Kesapragada, S. V.; Victor, P.; Nalamasu, O.; Gall, D. *Nano Lett.* **2006**, *6*, 854. (f) He, Y. P.; Fu, J. X.; Zhang, Y.; Zhao, Y. P.; Zhang, L. J.; Xia, A. L.; Cai, J. W. *Small* **2007**, *3*, 153. (g) Zhou, C. M.; Gall, D. *Appl. Phys. Lett.* **2006**, *88*, 203117. (h) Robbie, K.; Sit, J. C.; Brett, M. J. *J. Vac. Sci. Technol., B: Microelectron. Nanometer Struct.—Process., Meas., Phenom.* **1998**, *16*, 1115. (i) Vick, D.; Tsui, Y. Y.; Brett, M. J.; Fedosejevs, R. *Thin Solid Films* **1999**, *350*, 49.

Scheme 2. Schematic Illustration of Transferability of hcp Nanocolumn Arrays

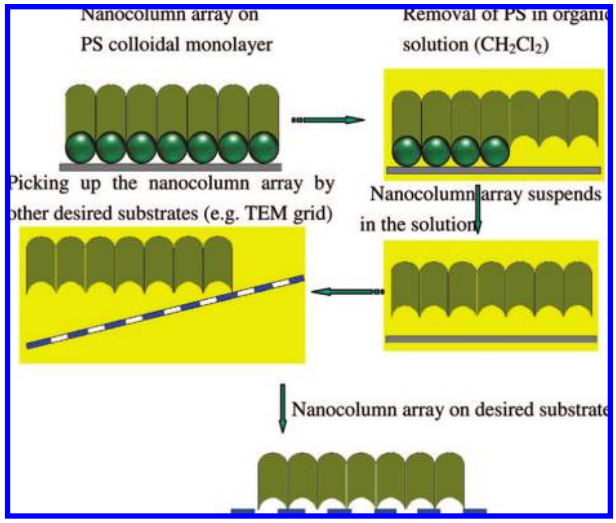

a small water droplet of 2 μL on this hierarchical nanocolumn array, the droplet spread out rapidly on the surface of the nanocolumn array and produced a flat water surface. The water CA became 0° in a short time (0.25 s) after the water was dropped onto the nanocolumn array, as seen in Figure 6. If a small oil droplet was placed on the nanocolumn surface, the same phenomenon occurred, and the oil CA became 0° in a short time (0.5 s) as indicated in Figure 7.

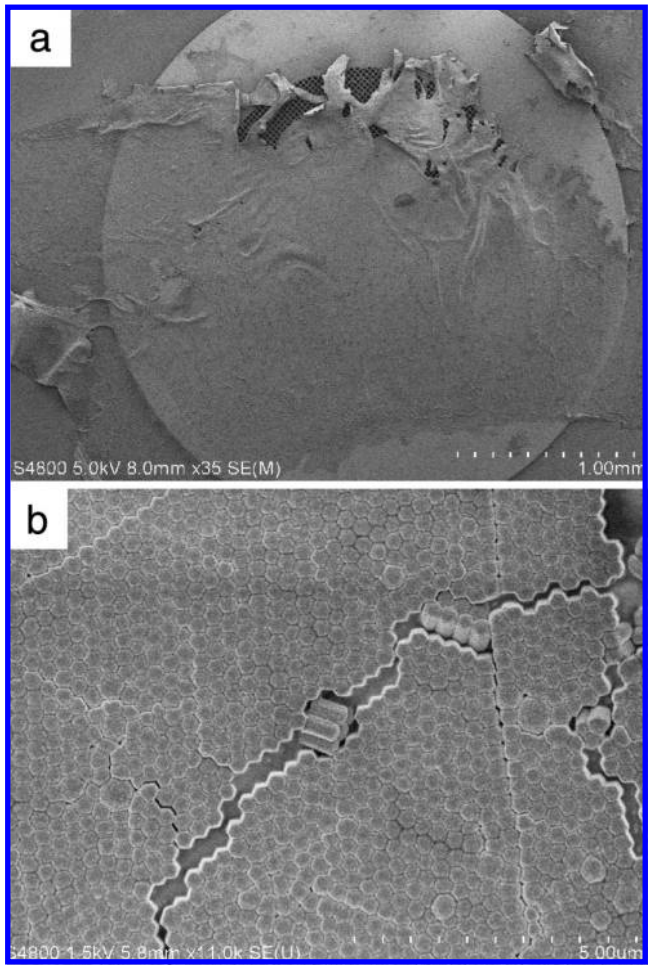

Figure 5. FE-SEM images of transferred nanocolumn arrays from a silicon substrate on a TEM grid. (a) Low- and (b) high-magnification images of nanocolumn array film on a TEM grid.

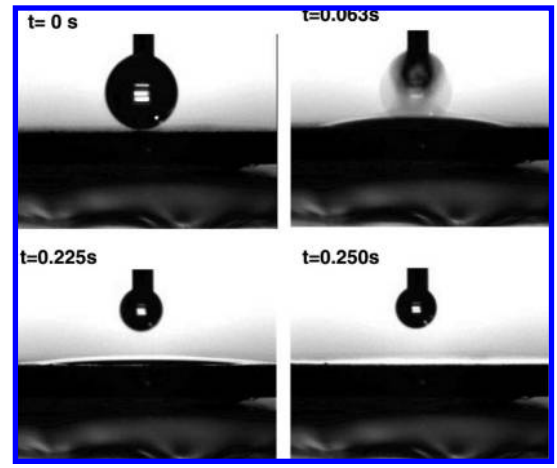

Figure 6. Time course of water-contacting behavior on the hcp hierarchical TiO_2 nanocolumn array film.

Figure 7. Oil (rapeseed) droplet shape on the nanocolumn array. The oil contact angle becomes 0° 0.5 s after it was dropped onto the surface.

Generally, a TiO_2 film with superamphiphilicity can be obtained by UV irradiation due to hydroxyls generated by oxygen defects and dangling bonds on its surface induced by photochemical processes. However, in our study, the as-prepared TiO_2 nanocolumn array film possessed superamphiphilicity without requiring further UV irradiation.

In the PLD process, a TiO_2 target is irradiated by a laser beam using energy exceeding its threshold, the ions (Ti^{4+}, O^{2-}, etc.) and electrons are released into the chamber, and some oxygen species are lost in the vacuum environment. Although oxygen is used as the background gas to supplement O elements in the deposition process, it is still easy to produce oxygen vacancies in the deposited TiO_2 during PLD, leading to the conversion of relevant Ti^{4+} sites to Ti^{3+} sites that are favorable for dissociative water adsoption.[22] These defect sites microscopically form hydrophilic domains, with sizes of several tens of nanometers, on the TiO_2 surface. However, the other parts of surface remain oleophilic, with fewer defects. Therefore, a composite TiO_2 surface having hydrophilic and oleophilic domains on a microscopically distinguishable scale was pro-

(22) (a) Hugenschmidt, M. B.; Gamble, L.; Campbell, C. T. *Surf. Sci.* **1994**, *302*, 329. (b) Henderson, M. A. *Surf. Sci.* **1996**, *355*, 151.

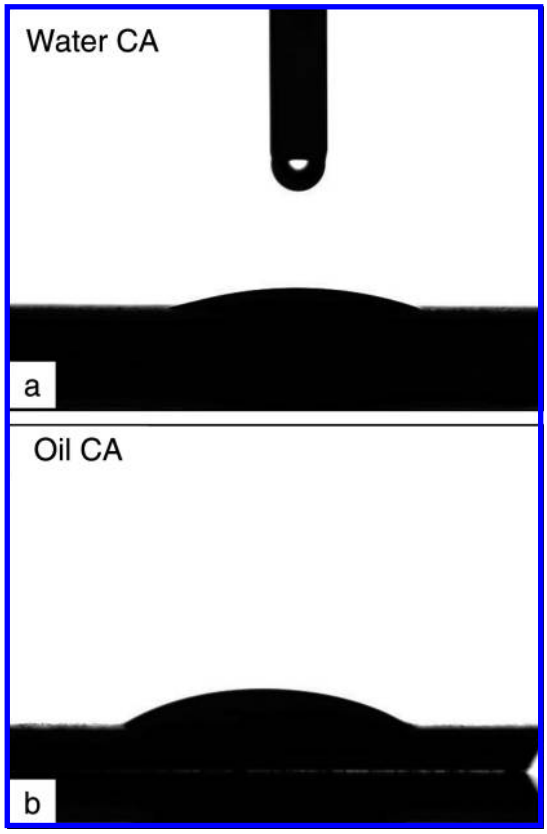

Figure 8. Photos for water contact angle measurement on a TiO_2 film on a silicon wafer prepared by PLD without using a PS colloidal monolayer. (a) Water CA: 15 degrees. (b) Oil (rapeseed) CA: 27 degrees.

duced. Such a composite surface macroscopically induced amphiphilicity on the TiO_2 surface, as Fujishima A. et al. reported.[23] A TiO_2 nanoparticle film without a PS colloidal monolayer was also prepared by PLD under the same experimental conditions as the hierarchical hcp nanocolumn array (Figure 4). The film top had almost the same particle size distribution as that of the hierarchical nanocolumn surface (Figure 1). The water CA of the film not using the PS colloidal monolayer was 15°, and the oil CA was about 27° (Figure 8). These results indicate that defect sites produced during PLD made the TiO_2 surface amphiphilic. Generally, the Wenzel mode is used to explain the wettability for a rough surface.[24]

$$\cos \theta_r = r \cos \theta \quad (1)$$

Here, r is the surface roughness, which is the ratio of total surface area to the projected area on the horizontal plane, and θ_r and θ are the CAs of a particle film and a native film with a smooth surface. This equation suggests that the wettability can be enhanced by increasing the surface roughness. Compared with the TiO_2 film (Figure 4) produced by PLD without using a colloidal monolayer, the hierarchical hcp TiO_2 nanocolumn array greatly increased the roughness of the TiO_2 surface, thereby enhancing the wettability from amphiphilicity to superamphiphilicity according to eq 1. The superamphiphilicity of the amorphous hierarchical hcp nanocolumn array originates

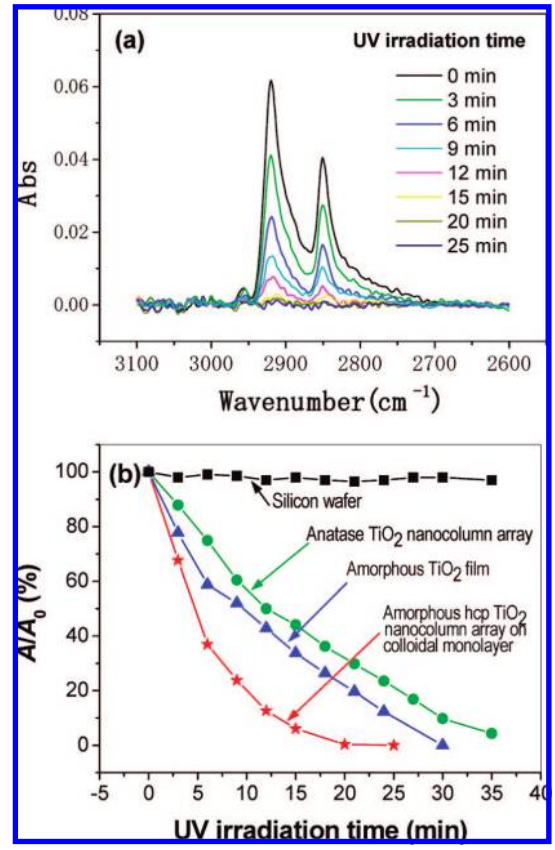

Figure 9. (a) Photocatalytic activity of an hcp amorphous TiO_2 nanocolumn array with a PS colloidal monolayer. (b) Photocatalytic activity evaluation of different substrates based on the absorbance ratio A/A_0 as a function of UV irradiation time. A and A_0 are the absorbance after the UV irradiation and that from the initial surface, respectively.

from the combination of the amphiphilicity produced by the PLD process and the special rough structures of hcp hierarchical nanocolumn arrays.

Enhanced Photocatalytic Activity. The photocatalytic activity of the as-prepared sample (hcp amorphous TiO_2 nanocolumn array on a colloidal monolayer) was estimated based on the decomposition of stearic acid under UV illumination by monitoring the FT-IR spectra (The UV−vis absorption spectrum indicated that the as-prepared sample had strong absorption in the UV range, as shown in Figure S4 of the Supporting Information).[25] The frequencies of 2919 and 2849 cm^{-1} indicate the methylene group asymmetric ($\nu_{asymmCH_2}$) and symmetric (ν_{symmCH_2}) stretching modes of stearic acid. These values for the methylene group stretching mode are close to those of a crystalline alkane and are typically taken as evidence of the formation of a dense, well-ordered, self-assembled monolayer of stearic acid on the oxide surface.[26] With increasing the UV illumination time, the vibrational bands of the methylene group gradually decreased and almost completely disappeared after 25 min, as shown in Figure 9a. The decrease in C−H vibrational bands indicates that the stearic acid is gradually photodegraded

(23) (a) Wang, R.; Hashimoto, K.; Fujishima, A.; Chikuni, M.; Kojima, E.; Kitamura, A.; Shimohigoshi, M.; Watanabe, T. *Nature* **1997**, *388*, 431. (b) Wang, R.; Hashimoto, K.; Fujishima, A.; Chikuni, M.; Kojima, E.; Kitamura, A.; Shimohigoshi, M.; Watanabe, T. *Adv. Mater.* **1998**, *10*, 135.
(24) Wenzel, R. N. *J. Phys. Colloid Chem.* **1949**, *53*, 1446.
(25) (a) Wang, K. X.; Yao, B. D.; Morris, M. A.; Holmes, J. D. *Chem. Mater.* **2005**, *17*, 4825. (b) Zhang, X. T.; Jin, M.; Liu, Z. Y.; Tryk, D. A.; Nishimoto, S.; Murakami, T.; Fujishima, A. *J. Phys. Chem. C* **2007**, *111*, 14521.
(26) (a) Gao, W.; Dickinson, L.; Grozinger, C.; Morin, F. G.; Reven, L. *Langmuir* **1996**, *12*, 6429. (b) Nuzzo, R. G.; Dubois, L. H.; Allara, D. L. *J. Am. Chem. Soc.* **1990**, *112*, 558. (c) Gawalt, E. S.; Avaltroni, M. J.; Koch, N.; Schwartz, J. *Langmuir* **2001**, *17*, 5736.

by the TiO_2 films under UV illumination. Figure 9b presents that degradation curves of a stearic acid film on a silicon wafer, an amorphous TiO_2 film by PLD without using a colloidal monolayer, an hcp amorphous TiO_2 nanocolumn array on the colloidal monolayer, and an anatase TiO_2 nanocolumn array (obtained by annealing hcp amorphous TiO_2 nanocolumn array on the colloidal monolayer at 650 °C for 2 h (Figure S5 of the Supporting Information)). From these results, it can be seen that TiO_2 exhibited efficient degradation for stearic acid and that the hcp amorphous TiO_2 nanocolumn array on a colloidal monolayer demonstrated the best performance compared to the amorphous film and the anatase nanocolumn array. Anatase is usually deemed to be more photocatalytically active than the rutile and amorphous TiO_2. However, besides the crystal phase, other factors, including the specific surface area, crystal composition, and material microstructures, also significantly affect the catalytic performance of TiO_2.[27] In our case, an amorphous hcp nanocolumn array has porous structures and possesses a much higher specific surface area than that of an anatase nanocolumn array, which contributes to better photocatalytic properties. Our results suggest that the surface area of TiO_2 is preferable to its crystal structure for enhancing photocatalytic activity. In addition, an ordered structured nanocolumn array of amorphous TiO_2 can enhance photocatalytic activity better than an amorphous TiO_2 thin film produced by PLD without using a colloidal monolayer. This may be ascribed to special hierarchical structures composed of radiation-shaped nanobranches emanating from a center point on the PS sphere.[28]

The combination of superamphiphilicity and photocatalytic activity is helpful in realizing a self-cleaning surface.[27] An oily liquid droplet placed on the as-prepared surface will spread out on the surface, becoming as large as possible, owing to superoleophilicity. This is useful for improving the photocatalytic efficiency if some amount of light illumination exists. Under UV irradiation or sunlight irradiation (sunlight contains some quantity of UV light, e.g. the UV light intensity is generally 2−3 mW cm^{-2} in direct sunlight in Japan), organic materials, including the oil, will gradually degrade. The contamination will be easily washed away from the surface by rainwater because of the superhydrophilicity, realizing a self-cleaning effect.

Conclusions

We present a new method of fabricating hcp hierarchical amorphous TiO_2 nanocolumn arrays by PLD, using a PS colloidal monolayer as a template. The nanocolumn array is formed by glancing deposition in multiple directions under the higher pressure of the background gas. The presented strategy is universal, permitting fabrication of nanocolumn arrays using different materials. The nanostructured array could be transferred to almost any desired substrate during the removal of the PS colloidal monolayer in an organic solution. The hierarchical TiO_2 nanocolumn array exhibits excellent superamphiphilicity without further UV irradiation and also demonstrates enhanced photocatalytic activity, causing the TiO_2 surface to readily realize a self-cleaning effect.

Acknowledgment. This work was supported by the Japan Society for the Promotion of Science (JSPS) fellowship. The authors are grateful to Dr. Haoshen Zhou, Dr. Eiji Hosono, Wataru Imano, and Dr. Hideo Tokuhisa from National Institute of Advanced Industrial Science and Technology for measuring the water contact angles and FT-IR spectra as well as for helpful discussions.

Supporting Information Available: Schematic illustration of PLD process (Figure S1); schematic illustration and results of multisubstrate experiments (Figures S2 and S2); UV−vis optical absorption of as-prepared sample (Figure S4); FE-SEM images, TEM image, and selected area electron diffraction pattern of a sample obtained by annealing an amorphous hcp TiO_2 nanocolumn array at 650 °C for 2 h in air (Figure S5). This material is available free of charge via the Internet at http://pubs.acs.org.

JA805077Q

(27) (a) Fujishima, A.; Zhang, X. T. *C. R. Chimie* **2006**, *9*, 750. (b) Macak, J. M.; Zlamal, M.; Krysa, J.; Schmuki, P. *Small* **2007**, *3*, 300. (c) Wu, C. Z.; Lei, L. Y.; Zhu, X.; Yang, J. L.; Xie, Y. *Small* **2007**, *3*, 1518.
(28) Li, H. X.; Bian, Z. F.; Zhu, J.; Zhang, D. Q.; Li, G. S.; Huo, Y. N.; Li, H.; Lu, Y. F. *J. Am. Chem. Soc.* **2007**, *129*, 8406.